PREPRINT: *Blocken B, Roels S, Carmeliet J. 2007. A combined CFD-HAM approach for wind-driven rain on building facades. Journal of Wind Engineering and Industrial Aerodynamics 95: 585-607. © Elsevier 2007.*

A combined CFD-HAM approach for wind-driven rain on building facades

Bert Blocken * [(a)], Staf Roels [(b)], Jan Carmeliet [(a,b)]

(a) Building Physics and Systems, Technische Universiteit Eindhoven, P.O. box 513, 5600 MB Eindhoven, The Netherlands
(b) Laboratory of Building Physics, Department of Civil Engineering, Katholieke Universiteit Leuven, Kasteelpark Arenberg 40, 3001 Leuven, Belgium

Abstract

Numerical Heat-Air-Moisture (HAM) transfer models are increasingly being used to study the hygrothermal performance and the durability of building facades. One of the most important boundary conditions for HAM simulations is wind-driven rain (WDR). Due to the complexity of WDR however, the current HAM models generally incorporate it in a very simplified way. Recent research has shown that CFD can provide quite accurate estimates of the spatial and temporal distribution of WDR on building facades. Therefore, in this paper, a combined CFD-HAM approach is presented. It consists of implementing catch-ratio charts resulting from CFD simulations into the HAM model. Within the model, these charts are used to convert the standard meteorological input data (wind speed, wind direction and horizontal rainfall intensity) into WDR distribution records that are used as boundary condition for the actual HAM simulations. The combined approach is demonstrated for a simplified wall model. It is shown that the accuracy of the HAM-simulation results is to a large extent determined by the time resolution of the meteorological input data and by the data-averaging technique used for these data. Some important guidelines for accurate HAM analyses with WDR are provided.

Keywords: Wind-driven rain; Driving rain; Wind flow; Building; Absorption; Runoff; Heat; Air; Moisture transfer analysis; HAM; Building; Computational Fluid Dynamics; Time resolution; Data averaging

1. Introduction

Numerical Heat-Air-Moisture (HAM) transfer models are an important tool to examine the hygrothermal behaviour and the durability of building facade components exposed to the outside climate. During the last decades, several HAM models have been developed and they have been progressively improved. An extensive survey of the state-of-the-art of these models was provided by Hens (1996) in the framework of the International Energy Agency Annex 24. Nowadays, several HAM models are commercially available and they are increasingly being used by a large number of researchers and building practitioners. Their capability is generally limited to HAM transfer in building components that are composed of isotropic, homogeneous materials. Currently, these models are in the process of becoming standardized procedures (CEN, 2003).

Accurate HAM-transfer analyses require adequate boundary conditions. Typically, the input of HAM models comprises a standard meteorological data record (containing air temperature, relative humidity, solar radiation, cloud factor, reference wind speed, wind direction and horizontal rainfall intensity) from which the specific boundary conditions are calculated. Although most boundary conditions can be quite adequately described for HAM-transfer analysis, there is at least one that is still considered to be problematic: wind-driven rain (WDR). Although WDR is generally considered to be one of the most important boundary conditions (Sanders, 1996; Dalgliesh and Surry, 2003; Blocken and Carmeliet, 2004) and it is expected to become even more important in the future (Sanders and Phillipson, 2003), its adequate implementation in HAM models has been held back by its complexity. WDR is highly variable in space and time because it is influenced by a variety of parameters, including the building geometry, the environment topology, the position on the building facade and the meteorological variables wind speed, wind direction and horizontal rainfall intensity, which are themselves complex functions of space and time. In order to provide HAM models with a suitable WDR boundary condition and to ensure the reliability of the HAM-simulation results, these models should comprise an adequate procedure

* Corresponding author: Bert Blocken, Building Physics and Systems, Technische Universiteit Eindhoven, The Netherlands. Tel.: +31 (0)40 247 2138; Fax +31 (0)40 243 8595; *E-mail address:* b.j.e.blocken@tue.nl

for calculating the quantity or intensity of WDR arriving at different positions on the building facade. This calculation should be performed based on the standard meteorological input variables: reference wind speed, wind direction and horizontal rainfall intensity.

Currently, two categories of methods exist for calculating the quantity or intensity of WDR based on standard meteorological data: (1) semi-empirical methods (such as the WDR relationship) and (2) numerical simulation methods based on Computational Fluid Dynamics (CFD). A review of these methods has been given by Blocken and Carmeliet (2004). At best, the currently existing HAM models employ the simple semi-empirical WDR relationship. Many researchers have employed this relationship and it is also the basis of the European Standard Draft PrEN13013-3 (Sanders, 1996; CEN, 1997; Blocken and Carmeliet, 2004) for WDR assessment. The reasons for its widespread use are: (1) it is very easy to implement (analytical formula); (2) its input are standard meteorological data that are generally available; and (3) no other suitable methods to determine WDR for real rain events have been available during the past decades. However, partly because of its simplicity, the WDR relationship can only provide rough estimates of WDR (Blocken and Carmeliet, 2004). In addition, recent research has shown that the WDR relationship is based on partially invalid assumptions that can give rise to significant errors (Blocken and Carmeliet, 2006a, 2006b; Janssen et al. 2006a).

In the past 15 years, CFD has made its introduction in the area of WDR research (Choi, 1991; 1993; 1994a; 1994b; Wisse, 1994; Lakehal et al., 1995; Karagiozis et al., 1997; van Mook et al., 1997; van Mook, 1999; 2002; Hangan, 1999; Etyemezian et al., 2000; Blocken and Carmeliet, 2002; 2004; 2006c; Tang and Davidson 2004). In a few of these publications the authors explicitly stated that their research was driven by the need for adequate WDR boundary conditions for HAM simulations (Karagiozis et al., 1997; van Mook, 2002; Blocken and Carmeliet, 2002; 2004; Tang and Davidson, 2004). Also Dalgliesh and Surry (2003) mentioned the possibility of using CFD for this purpose. Recently, the use of CFD for WDR modelling based on meteorological data records has been successfully validated for the case of a low-rise building of complex geometry (Blocken and Carmeliet 2002; 2004; 2005; 2006c) and for a high-rise building (Tang et al., 2004; Tang and Davidson, 2004), in both cases for a range of different rain events. CFD modelling of WDR allows overcoming the drawbacks of the WDR relationship. It can be used to provide more detailed and accurate estimates of the spatial and temporal distribution of WDR on building facades than the semi-empirical WDR relationship.

In this paper, a combined CFD-HAM approach is presented. This approach is based on catch-ratio charts that are generated from CFD simulation results and that are implemented in the HAM model. The combined approach is applied for a simple, fictitious, two-layer porous wall configuration and for two different rain events. The focus is on the moisture behaviour of the wall. Because of its importance, the influence of the time resolution of the standard wind and rain data and of different averaging techniques for these data on the moisture behaviour is specifically investigated. First, in section 2, the numerical WDR model (CFD), the HAM model and the way in which they are combined are described. In section 3, the combination of both is applied to study the moisture behaviour of the wall configuration. Section 4 and section 5 respectively outline the limitations of this research and the conclusions.

2. Numerical models

2.1. Wind-driven rain model

In this subsection, the WDR model is briefly outlined. First, a few definitions and the influencing parameters of WDR are given. Next, the simulation methodology (5-step method) is described and the validation of the WDR model is briefly addressed. Finally, the two averaging techniques that will be applied to the input wind and rain data – the traditional one and a new technique – are given.

2.1.1. Definitions and parameters

The quantities that are used to describe the WDR intensity are the specific catch ratio $\eta_d(d,t)$, related to the raindrop diameter d, and the catch ratio $\eta(t)$, related to the entire spectrum of raindrop diameters (Eq. 1):

$$\eta_d(d,t) = \frac{R_{wdr}(d,t)}{R_h(d,t)} \quad ; \quad \eta(t) = \frac{R_{wdr}(t)}{R_h(t)} \tag{1}$$

where $R_{wdr}(d,t)$ and $R_h(d,t)$ are the specific WDR intensity on the building and the specific unobstructed horizontal rainfall intensity, respectively. $R_{wdr}(t)$ and $R_h(t)$ respectively refer to the same quantities but integrated over all raindrop diameters. The unobstructed horizontal rainfall intensity is the intensity of rainfall through a horizontal plane that is situated outside the wind-flow pattern that is disturbed by the building. The catch ratio η is a complex function of space and time. The six basic influencing parameters for η are: (1) the building geometry (including environment topology), (2) the position on the building facade, (3) the reference wind

speed, (4) the reference wind direction, (5) the horizontal rainfall intensity and (6) the horizontal raindrop-size distribution. The reference wind speed U (m/s) is usually taken as the horizontal component of the wind-velocity vector at 10 m height in the upstream undisturbed flow (U_{10}). The reference wind direction φ_{10} (degrees from north) refers to the direction of the reference wind speed. The horizontal raindrop-size distribution $f_h(d)$ (m^{-1}) refers to the raindrop-size distribution as a flux through a horizontal plane (Blocken and Carmeliet 2002, 2004).

2.1.2. Five-step simulation methodology

The numerical methodology for determining the spatial and temporal distribution of WDR on buildings consists of 5 steps and is based on the steady-state simulation procedure developed by Choi (1991; 1993; 1994a) (steps 1 – 4) and on the extension of this procedure into the temporal domain by Blocken and Carmeliet (2002) (step 5):

1. The steady-state 3D wind-flow pattern around the building is calculated using a CFD code. Usually, the Reynolds-Averaged Navier-Stokes (RANS) equations are solved and closure is obtained by employing a turbulence model.
2. Raindrop trajectories are obtained by injecting raindrops of different sizes in the calculated wind-flow pattern and by solving their equations of motion.
3. The specific catch ratio is determined based on the configuration of the calculated trajectories that end on the building facade.
4. The catch ratio is calculated from the specific catch ratio and from the raindrop-size distribution, for a range of reference wind speed values and horizontal rainfall intensities.
5. Based on the calculated catch ratios, catch-ratio charts are constructed. Each chart displays the catch ratio η as a function of the reference wind speed U_{10} and the horizontal rainfall intensity R_h for a given position on the facade and for a given wind direction. An example of a catch-ratio chart is given in Fig. 1. Once the catch-ratio charts have been constructed for a certain building configuration, they can be used to rapidly convert any meteorological data record of reference wind speed, wind direction and horizontal rainfall intensity into the corresponding WDR records on the building facade. The procedure is as follows. To determine the WDR record for a rain event, this event is partitioned into a number of equidistant time steps (e.g. 10-minute intervals). Each time step is considered steady-state and the standard meteorological data for each time step are used to extract the corresponding catch ratio from the appropriate catch-ratio chart. Multiplying the catch-ratio value for a time step with the corresponding horizontal rainfall amount S_h for that time step yields the WDR amount for that time step: S_{wdr}.

2.1.3. Validation

The numerical WDR simulation model, including all five steps mentioned above, has been validated in earlier studies based on full-scale WDR measurements on a low-rise building (Blocken and Carmeliet 2002, 2004, 2005, 2006c). It has been shown that the spatial and temporal distribution of WDR on the facade of a low-rise building can be calculated with fairly good accuracy for a range of different rain events. Note that the validation studies were limited to wind directions that were approximately perpendicular to the facade under study. The reason is that full-scale WDR measurements can suffer from significant errors for oblique wind directions because of the wind error, rendering them less useful for model validation. The wind error is expected to become more important as the angle of wind becomes more oblique to the facade. The wind error and errors in WDR measurements in general are addressed in (Blocken and Carmeliet, 2005; 2006b). Because the validation was limited to wind directions that are approximately perpendicular to the facade, the combined CFD-HAM approach in this paper will also only be applied for wind direction perpendicular to the facade and for the same low-rise test building for which the validation was conducted.

2.1.4. Time resolution and data averaging

Earlier research has indicated the importance of the time resolution of the input wind and rain data that are needed in step 5 of the numerical WDR model (Blocken and Carmeliet, 2000). It has been demonstrated that the use of 1-minute or 10-minute data can yield accurate results (Blocken and Carmeliet, 2002; 2006c). However, most climatic databases in general and HAM-model climatic databases in particular contain data on – at best – an hourly basis. These data have typically been obtained by averaging short-term data (e.g. 1-minute or 10-minute data) from meteorological stations over hourly intervals with the standard arithmetic-averaging technique (e.g. Eq. (2) for averaging wind speed and horizontal rainfall intensity data):

$$U_j = \frac{\sum_i U_i}{n} \quad ; \quad R_{hj} = \frac{\sum_i R_{h_i}}{n} \tag{2}$$

In Eq. (2), the index j refers to the hourly value, the index i refers to the short-term values (e.g. 1-minute or 10-minute) within this hour, n is the number of short-term time steps in one hour and the summation extends over all short-term time steps in the hour.

Up to now, hourly data have been considered suitable for most HAM simulations (Künzel, 1993; Geving, 1994; 1997). However, previous studies on the influence of the time resolution of the input data on the HAM results were focused on the difference between results obtained with hourly, daily, monthly and six-monthly data. They did not evaluate data at a smaller time scale than hourly. Neither did they focus on WDR as a boundary condition. In this respect, it is important to note that Hens (1996) correctly mentions that hourly data may not be good enough when precipitation data are to be included in HAM simulations.

Concerning WDR, validation studies of CFD simulations have shown that accurate WDR results can be obtained from 1-minute or 10-minute data of wind speed, wind direction and rainfall intensity (Blocken and Carmeliet, 2002; 2006c) and that the use of hourly data obtained by arithmetic averaging (standard practice) can yield significant underestimations in the calculated WDR amounts (Blocken and Carmeliet, 2000). On the other hand, the use of hourly data can provide good results if they have been obtained from averaging short-term data with a new weighted data-averaging technique, where the horizontal rainfall amounts S_{hi} for each time step are used as weighting factors: Eq. (3):

$$U_j = \frac{\sum_i U_i S_{hi}}{\sum_i S_{hi}} \quad ; \quad R_{hj} = \frac{\sum_i R_{hi} S_{hi}}{\sum_i S_{hi}} \tag{3}$$

The errors in the calculated WDR amounts that are due to inappropriate time resolution or data averaging with Eq. (2) will evidently be transferred to the HAM-simulation results. The effects on the accuracy of these results will be investigated in section 3 of this paper.

2.2. Heat and moisture transfer model for the building facade

The common way to model transport phenomena in media with a complex microscopic pore structure is the continuum approach (Bear and Bachmat, 1975; Whitaker, 1977). Continuum modelling assumes that the physical properties of the porous medium can be associated with mathematical field variables, whose time and space dependencies are represented in the form of differential balance equations for mass, momentum and energy. Inherently, the continuum approach is a phenomenological approach whereby capacity and transport properties are determined experimentally. Since the focus in this paper is on the WDR boundary condition, air transport will be neglected. Hence, the HAM model reduces to a heat and moisture transfer model and the governing equations can be written as:

$$c\rho_0 \frac{\partial T}{\partial t} + \nabla\left(q_{cond} + q_{conv}\right) = 0 \tag{4}$$

$$\xi \frac{\partial p_c}{\partial t} + \nabla\left(g_v + g_l\right) = 0 \tag{5}$$

The first equation describes the conservation of energy, where ρ_0 is the dry density of the material and where c is a lumped capacity term, accounting for the heat capacity of both bulk material and of air, water and vapour present in the pores of the material. T is the temperature, t the time co-ordinate, ∇ the divergence operator and q_{cond} and q_{conv} respectively describe the heat flow rate by conduction and by convection. The latter represents convective heat flows due to vapour and liquid flow including latent heat transport. The second equation is the moisture balance equation in which the capillary pressure p_c is taken as basic variable. ξ represents the moisture capacity, i.e. the derivative of the moisture-retention curve giving the moisture content w as a function of the capillary pressure p_c. Moisture is transported in either vapour or liquid phase. The respective flow rates are denoted as g_v and g_l. While the liquid part is only weakly influenced by a temperature gradient, the vapour flow rate is strongly dependent on the temperature gradient. In non-isothermal conditions it is therefore necessary to account for two independent state variables: p_c and T. The elaborated version of the governing equations can be found in e.g. (Bear and Bachmat, 1975; Whitaker, 1977).

In the mathematical model boundary conditions have to be imposed. The heat flux q_n at the exterior wall surface (boundary) can be simplified as:

$$q_n = h\,(T^{eq} - T_{surf}) + g_{v,n}\,\ell_{\ell v} + g_{\ell,n} c_\ell\, T_{wdr} \tag{6}$$

and the heat flux at the interior wall surface (boundary) can be written as:

$$q_n = h\,(T_a - T_{surf}) + g_{v,n}\,\ell_{\ell v} \tag{7}$$

In these equations, the first term accounts for both convective and short and long-wave radiative exchange with the surroundings by means of an effective heat-transfer coefficient h and an equivalent temperature T^{eq} (for outside) or an inside temperature T_a (for inside). T_{surf} is the temperature at the wall surface. The second term covers the latent heat transfer with l_{lv} the specific enthalpy of evaporation. The last term in Eq. (6) covers the heat transfer due to liquid inflow $g_{l,n}$, with c_l the specific heat capacity of water and T_{wdr} the temperature of the rainwater. The moisture fluxes $g_{v,n}$ and $g_{l,n}$ at the boundary can be written as:

$$g_{v,n} = \beta\,(p_a - p_{surf}) \tag{8}$$

$$g_{\ell,n} = \max\left(R_{wdr}, k\frac{\partial p_c}{\partial n}\right) \tag{9}$$

with β the surface vapour-transfer coefficient, p_a the vapour pressure in the air and p_{surf} the vapour pressure at the surface. Note that we limit the moisture content in the material to the capillary moisture content, which in turn limits the liquid inflow: the liquid flux as provided by WDR is the maximum value of two variables; it can be taken as a prescribed liquid flux boundary condition that is equal to R_{wdr} as long as the moisture content at the exterior surface remains below the capillary moisture content. Once the capillary moisture content is reached (i.e. the exterior surface is capillary saturated with water), the liquid inflow reduces to $k(\partial p_c / \partial n)$, where k is the moisture permeability. At that moment, the excess of rainwater runs down the wall (runoff).

2.3. Combined CFD-HAM approach

The combination of CFD and HAM modelling is established based on the catch-ratio charts that are generated from the CFD simulation results. The catch-ratio charts are implemented in the HAM model. The advantage of these charts is that, once they have been generated, they provide a very fast and easy way to convert any standard meteorological data record (containing reference wind speed, wind direction and horizontal rainfall intensity) into the corresponding WDR records for different positions at the building facade. The WDR records are used as boundary condition for the actual HAM calculations that provide information about the HAM transfer in and through the facade.

3. Numerical simulations and results

3.1. General

The combined CFD-HAM approach is applied for a simple wall model for two reasons: (1) to illustrate the performance of the combined approach; (2) to specifically investigate the influence of the following aspects on the predicted moisture behaviour: (a) The time resolution of the meteorological input data (10-minute versus hourly data) and (b) The averaging technique used to convert the 10-minute meteorological input data to hourly meteorological data (arithmetic versus weighted averaging). This investigation is important because the current meteorological databases for HAM studies typically consist of hourly, arithmetically-averaged meteorological data.

The study is performed for two different rain events: a cumuliform rain event and a stratiform rain event. The terminology “cumuliform-stratiform” stems from the type of clouds generating the rain. *Cumuliform clouds* or heap clouds (Fig. 2a) develop in an unstable atmosphere as a result of fast and local rising air currents. The type of rainfall from these clouds is referred to as showers (Fig. 2b). Showers usually start and stop suddenly and are generally of short duration. *Stratiform clouds* or layer clouds (Fig. 2c) develop in a stable atmosphere as a result of widespread cooling and by condensation processes that are slow but persistent. The precipitation from these clouds starts and stops slowly, is quite steady (although it can exhibit breaks), often lasts for many hours and is generally of light to moderate intensity ($R_h < 7.6$ mm/h) (Fig. 2d).

3.2. Building model, wall model and material characteristics

The building model is the VLIET test building of the Laboratory of Building Physics, situated at the K.U.Leuven University Campus. The building and the associated measurement set-up for wind, rain and WDR are described in detail in (Blocken and Carmeliet, 2005). The VLIET building is chosen for this study because the CFD simulation model for WDR was applied and validated for this particular building in previous work (Blocken and Carmeliet, 2002; 2006c). Figure 3 illustrates the north-west and the south-west facade of the building, including the main dimensions and roof overhang lengths. In this study, we focus on two positions on the south-west facade: A and B.

The 1D wall model and the material characteristics for this study have been taken equal to those used for one of the benchmarks in the European project HAMSTAD (Heat Air and Moisture STAndards Development) (Hagentoft et al., 2004). The wall model of the benchmark is illustrated in Fig. 4. It is a simple two-layer wall: the outer layer is made of ceramic brick, the inner layer is plaster. The moisture retention curve $w(p_c)$ and the liquid and vapour permeability curves of the ceramic brick are given in Fig. 5 and 6. For a detailed description of all material characteristics, the reader is referred to Hagentoft et al. (2004). In the simulations reported below, we will consider the fictitious situation in which this two-layer wall model represents the south-west facade of the VLIET building.

3.3. Initial and boundary conditions

The boundary conditions for the model are illustrated in Fig. 4 and are listed, together with the initial conditions, in Table 1 (except for the WDR boundary condition). In Table 1, p_c is the capillary pressure in the brick wall, T_e and T_i are the exterior and interior air temperature, h_e and h_i are the exterior and interior surface heat-transfer coefficient, p_e and p_i are the exterior and interior vapour pressure, β_e and β_i are the exterior and interior surface vapour-transfer coefficient, T_{wdr} is the temperature of the rain water and R.H. stands for relative humidity. To focus on the effect of the WDR boundary condition, the other boundary conditions are kept constant. The WDR boundary condition will be provided in subsection 3.5, together with the HAM simulation results.

3.4. Modelling assumptions

The following assumptions for the calculations are made:

1. The wind direction during the rain events is south-west, i.e. perpendicular to the south-west building facade (Fig. 3).
2. The materials are homogeneous and isotropic.
3. For simplicity, only heat and moisture (vapour + liquid) transfer are simulated. No air transfer takes place through the wall.
4. All WDR falling on the outer surface of the wall is taken up by the material (it is modelled as a water flux). Therefore it is assumed that splashing as well as runoff is neglected. The first assumption will be approximately valid when the wind speed and horizontal rainfall intensity are low (Blocken and Carmeliet, 2006b). The second assumption holds as long as the outer surface does not reach the capillary moisture content. This will be the case in all simulations presented below.
5. The temperature of the rainwater is equal to the outside air temperature. This information is needed because WDR, besides a moisture flux, is also an enthalpy flux (Eq. 6).

3.5. Simulation results

In discussing the simulation results, we will focus on two aspects of the moisture behaviour of the wall: the moisture content at the outer surface and the spatial average of the moisture content in the ceramic brick wall. The former is important because it is an indication of when runoff might occur (which happens when the moisture content w at the surface reaches the capillary moisture content w_{cap}), the latter is important because it governs most moisture-related damage mechanisms in porous building materials.

3.5.1. Cumuliform rain event

Fig. 7a illustrates the cumuliform rain event. Figs. 7b-c show the corresponding results for the temporal distribution of the cumulative WDR amount at positions A and B of the facade. This distribution was obtained based on the catch-ratio charts that were generated by the CFD model. The WDR amount has been calculated in three ways:

1. Based on 10-minute data of U_{10} and R_h, yielding 10-minute WDR values (these values are considered as the reference solution).
2. Based on arithmetically-averaged hourly data of U_{10} and R_h, yielding 1-hour WDR values, denoted with "ar.avg" (standard practice).

3. Based on weighted-averaged hourly data of U_{10} and R_h, yielding 1-hour WDR values, denoted with "w.avg" (new technique).

Figs. 7b-c show that:

1. The arithmetically-averaged hourly data considerably underestimate the WDR amount.
2. The weighted-averaged hourly data provide a very good correspondence with the reference solution.

These data have been used as a boundary condition for the HAM simulations.

Figs. 8a-b illustrate the moisture content at the outer surface of the brick wall for position A and B. It is clear that the occurrence of WDR leads to pronounced peaks in the moisture content at the surface. After the occurrence of WDR, these peaks fade out due to the combination of drying and moisture redistribution into the wall. The following observations are made from the figures:

1. The 10-minute data clearly yield larger peak-moisture-content values at the surface than the hourly data. This is partly caused by the fact that the WDR amount is spread equally over the time interval as a boundary condition in the heat and moisture transfer simulation (10 minutes versus 1 hour). As a result, peak values are flattened. An example of this situation is an hourly interval in which it rains only in one of the six 10-minute intervals.
2. The arithmetic-averaging technique not only causes an additional suppression of the peak values, it also shows a general poor performance during the entire rain event. Note that the first peak value at position A is not reproduced at all (due to the combination of arithmetic averaging and the effect of roof overhang).
3. The hourly WDR data "w.avg" that result from the weighted-averaging technique show a significantly better performance. Note that they do not accurately reproduce the peak values but that for the remainder of the plot, the correspondence with the 10-minute results is good.

Figs. 9a-b illustrate the mean moisture content in the brick layer. The following observations are made:

1. The results from the 10-minute WDR data and the "w.avg" hourly WDR data show a good agreement. Only some minor discrepancies are noted during the course of the rain event.
2. The "ar.avg" hourly WDR data provide a large underestimation of the mean moisture content, which could be expected given the large underestimation error indicated in Figs. 7b-c.

3.5.2. Stratiform rain event

Fig. 10a illustrates the stratiform rain event. Figs. 10b-c show the corresponding temporal distribution of the cumulative WDR amount at position A and B of the facade. The WDR amount has been calculated using the same three procedures as described above: "10 min.", "ar.avg" and "w.avg". Both figures show that all results are almost equal. The close agreement is due to the stratiform character of the rain event: the fluctuations in wind speed (during rain) and horizontal rainfall intensity are considerably less pronounced than for the cumuliform rain event which limits the errors due to data-averaging (Blocken and Carmeliet, 2000).

Figs. 11a-b illustrate the moisture content at the outer surface of the brick wall for position A and B:

1. The 10-minute data yield larger peak-moisture-content values at the surface than the hourly data, for the same reason as mentioned in subsection 3.5.1.
2. Except for the peak value in the beginning of the rain event, all three sets of WDR data yield similar results.

Figs. 12a-b illustrate the mean moisture content in the brick layer. The agreement between the results is very good.

4. Limitations of this research

It is important to mention the limitations of this research work:

1. The homogeneous, isotropic two-layer wall model is a simplified and theoretical example. The reality is often much more complex. In the case of brickwork, the brick-mortar interface, cracks and joints are important features that govern rain penetration and in a full HAM-transfer modelling study, their effects should be taken into account. Important steps to take into account these effects have only quite recently been established (e.g. Wilson et al., 1995; Brocken, 1998; Roels et al., 2003; Carmeliet et al., 2004) and further research on this matter is ongoing. It is important to note that the use of a simplified wall model in this study does neither detract from its importance, nor does it influence the conclusions that will be made in the next section. After all, also in walls consisting of heterogeneous, non-isotropic materials, accurately modelling the WDR boundary condition and capillary uptake by WDR – as addressed in this paper – is an essential prerequisite for adequate and accurate results.
2. In the present paper, the focus was on the WDR boundary condition and for clarity all other boundary conditions were kept constant. It is clear that the moisture response of a facade will be strongly influenced by variations in the other boundary conditions as well (Janssen et al., 2006a). Furthermore, it was assumed that the response of the wall only consisted of taking up all WDR falling onto the building facade by capillary absorption (including evaporation). This is a good approximation for the material characteristics and the low

WDR exposure considered in this study. Generally however, the response of the wall can also be governed by other contact and surface phenomena that occur when raindrops hit a vertical wall (splashing, adhesion, runoff). Especially rainwater runoff is important. It constitutes an additional and important moisture source for the lower parts of the facade (it might just as well be the only moisture source at these positions, see (Blocken and Carmeliet, 2006c)) and it is one of the main mechanisms governing rain penetration. In addition, it is responsible for the surface soiling patterns on building facades (white-washing and dirt-washing) that have become characteristic for so many of our buildings.

3. Two individual rain events have been considered in this study. The significance of the underestimations that will occur in reality depends to a large extent on the amount of cumuliform versus stratiform rain events in a year. This amount can be very different depending on the climate. For example, data analysis by the authors has shown that Flanders and the Netherlands (climate type "Cf") have a majority of stratiform rain events, while others mention that Singapore (climate type "Af") has more than 200 cumuliform thunderstorms a year (Choi, 2001). The indication of the climate types is according to the Köppen Climate Classification System (Strahler and Strahler, 1984). The letters in the classification refer to the main climate type and the subtype(s). "C" refers to a "Humid Middle Latitude Climate" while "A" indicates a "Moist Tropical Climate". The second letter "f" refers to a climate that is "moist with adequate precipitation in all months and no dry season". In "Af" climates, due to high surface heat and humidity, cumuliform clouds form early in the afternoons almost every day. Especially in such climates, using an appropriate time resolution and/or the new weighted averaging technique is very important.

5. Conclusions

A combined CFD-HAM approach for WDR on building facades has been presented. This approach is based on catch-ratio charts that are generated from CFD simulation results. The catch-ratio charts are implemented in the HAM model. Once they have been generated, they provide a very fast and easy way to convert any standard meteorological data record (containing reference wind speed, wind direction and horizontal rainfall intensity) into the corresponding WDR records for different positions at the building facade. The WDR records are used as boundary condition for the actual HAM calculations.

The combined approach has been applied for a simple, fictitious, two-layer porous wall configuration and for two different rain events. The influence of the time resolution of the input standard wind and rain data and the effect of using different averaging techniques for these data on the moisture behaviour have been investigated. The following conclusions can be made:

1. The magnitude of the errors introduced by low time resolution data (e.g. hourly) and by data averaging is strongly dependent on the type of rain event. For cumuliform rain events, which are characterized by highly fluctuating wind speed and horizontal rainfall intensity, the errors can be quite large. For stratiform rain events, which are characterized by much smaller temporal variations in wind and rain characteristics, the errors are significantly smaller. The errors in the WDR data are evidently passed on to the predicted moisture behaviour of the wall.
2. The use of hourly WDR data can significantly underestimate the peak values of surface moisture content. Hourly WDR data, no matter how they have been obtained, are generally not suitable for HAM simulations when predicting the surface moisture content is important (e.g. in studies of rainwater runoff). Given the possibility of a high temporal variability of the horizontal rain intensity, even 10-minute data may not be good enough. This is a reason for concern, given the fact that most meteorological databases contain – at best – hourly data.
3. The use of hourly meteorological data is appropriate for the calculation of the mean moisture content, on condition that they have been obtained by weighted averaging and not by arithmetic averaging. Again, this is a reason of concern: almost all meteorological databases contain arithmetically-averaged data (standard practice).
4. The importance and the frequency of occurrence of errors due to time resolution and averaging are to a large extent determined by the climate type, more specifically by the amount of cumuliform versus stratiform rain events. Especially for climates with a significant number of cumuliform rain events, using an appropriate time resolution and/or the new weighted averaging technique is very important. Investigating the importance of the climate type is an important subject of future research.

As a result of this research, CFD catch-ratio charts for different building configurations (Blocken and Carmeliet, 2006c) have been implemented in the HAM-software HAMFEM of the Laboratory of Building Physics (Janssen et al., 2006a; 2006b) to replace the semi-empirical WDR relationship. The next generation of HAM simulations at the Laboratory are based on these and future CFD-generated data for WDR. Nevertheless, it should be noted that the research reported in this paper is not complete; it is a first step towards combined CFD-HAM modelling. Further research needs include additional validation studies of WDR for different building

configurations and the establishment of high-quality WDR experimental databases to allow such validation efforts. Future research should also focus on the study of contact and surface phenomena in general, on rainwater runoff in particular and on the comparison of HAM simulations with full-scale experimental data. These studies are an essential prerequisite to arrive at an elaborate combined CFD-HAM approach for WDR on building facades.

Acknowledgements

This research was conducted while the first author was a post-doctoral research fellow of the FWO-Flanders. The FWO-Flanders (Research Fund – Flanders) supports and stimulates fundamental research in Flanders (Belgium). Their financial contribution is gratefully acknowledged. The authors also express their gratitude for the financial support from the Katholieke Universiteit Leuven (KUL-OT 04/28: "Towards a reliable prediction of the moisture stress on building enclosures").

Nomenclature

a	index for air
c	specific heat capacity (J/kgK)
$f_h(d)$	probability-density function of raindrop size as a flux through a horizontal plane (m^{-1})
g	density of moisture flow rate (kg/m²s)
h_e, h_i	surface heat-transfer coefficient (e = exterior, i = interior) (W/m²K)
i	index that refers to short-term meteorological data
j	index that refers to long-term (averaged) meteorological data
k	moisture permeability (s)
l	index that refers to liquid
l_{lv}	specific enthalpy of evaporation (J/kg)
n	number of time steps
n	index that refers to the normal to the boundary
p_c	capillary pressure (Pa)
p_e, p_i	vapour pressure (e = exterior, i = interior) (Pa)
q	density of heat flow rate (W/m²)
R_h	horizontal rainfall intensity, i.e. through a horizontal plane (L/m²h or mm/h)
R_{wdr}	wind-driven rain intensity (L/m²h or mm/h)
R.H.	relative humidity (%)
S_h	horizontal rainfall amount, i.e. through a horizontal plane (L/m or mm)
S_{wdr}	wind-driven rain amount (L/m or mm)
T_e, T_i	temperature (e = exterior i = interior) (K)
T_{wdr}	temperature of the wind-driven rain water (K)
U	streamwise horizontal component of the mean wind-velocity vector (m/s)
U_{10}	reference wind speed at 10 m height in the upstream undisturbed flow (m/s)
v	index that refers to vapour
w	moisture content (kg/m³)
w_{cap}	capillary moisture content (kg/m³)
x, z	streamwise and spanwise co-ordinate (m)
y	height co-ordinate (m)
β_e, β_i	surface vapour-transfer coefficient (e = exterior, i = interior) (s/m)
η_d	specific catch ratio (-)
η	catch ratio (-)
ρ	density (kg/m³)
ξ	moisture capacity (kg/m³Pa)
φ_{10}	wind direction at 10 m height in the upstream undisturbed flow (degrees from north)
CFD	Computational Fluid Dynamics
HAM	Heat-Air-Moisture
VLIET	VLaams Impuls programma voor EnergieTechnologie (Flemish Impulse Programme for Energy Technology)
WDR	Wind-Driven Rain

References

Bear, J., Bachmat, Y., 1975. Introduction to modelling of transport phenomena in porous media. Kluwer Academic Publishers, Dordrecht.

Blocken, B., Carmeliet, J., 2000. Driving rain on building envelopes – II: representative experimental data for driving rain estimation. Journal of Thermal Envelope and Building Science 24(2), 89-110.

Blocken, B., Carmeliet, J., 2002. Spatial and temporal distribution of driving rain on a low-rise building. Wind and Structures 5(5), 441-462.

Blocken, B., Carmeliet, J., 2004. A review of wind-driven rain research in building science. Journal of Wind Engineering and Industrial Aerodynamics 92(13), 1079-1130.

Blocken, B., Carmeliet, J., 2005. High-resolution wind-driven rain measurements on a low-rise building. Journal of Wind Engineering and Industrial Aerodynamics 93(12), 905-928.

Blocken, B., Carmeliet, J., 2006a. On the validity of the cosine projection in wind-driven rain calculations on buildings. Building and Environment 41(9), 1182-1189.

Blocken, B., Carmeliet, J., 2006b. On the accuracy of wind-driven rain measurements on buildings. Building and Environment 41(12), 1798-1810.

Blocken, B., Carmeliet, J., 2006c. The influence of the wind-blocking effect by a building on its wind-driven rain exposure. Journal of Wind Engineering and Industrial Aerodynamics 94(2), 101-127.

Brocken, H.J.P., 1998. Moisture transport in brick masonry: the grey area between the bricks. Ph.D. thesis, Building Physics and Systems, Technische Universiteit Eindhoven, The Netherlands.

Carmeliet, J., Delerue, J.F., Vandersteen, K., Roels, S., 2004. Three-dimensional liquid water transport in concrete cracks. International Journal for Numerical and Analytical Methods in Geomechanics 28(7-8), 671-687.

CEN, 1997. Hygrothermal performance of buildings – Climatic data – Part 3: Calculation of a driving rain index for vertical surfaces from hourly wind and rain data. Draft prEN 13013-3.

CEN, 2003. Hygrothermal performance of building components and building elements – assessment of moisture transfer by numerical simulation. CEN/TC 89 WI29.3. Working Document for European Standard.

Choi, E.C.C., 1991. Numerical simulation of wind-driven-rain falling onto a 2-D building, in: Proceedings of Asia Pacific Conference on Computational Mechanics, Hong Kong, 1721-1728.

Choi, E.C.C., 1993. Simulation of wind-driven rain around a building. Journal of Wind Engineering and Industrial Aerodynamics 46&47, 721-729.

Choi, E.C.C., 1994a. Determination of wind-driven rain intensity on building faces. Journal of Wind Engineering and Industrial Aerodynamics 51, 55-69.

Choi, E.C.C., 1994b. Parameters affecting the intensity of wind-driven rain on the front face of a building. Journal of Wind Engineering and Industrial Aerodynamics 53, 1-17.

Choi, E.C.C., 2001. Wind-driven rain and driving rain coefficient during thunderstorms and non-thunderstorms. Journal of Wind Engineering and Industrial Aerodynamics 89, 293-308.

Dalgliesh, W.A., Surry, D., 2003. BLWT, CFD and HAM modelling vs. the real world: Bridging the gaps with full-scale measurements. Journal of Wind Engineering and Industrial Aerodynamics 91(12-15), 1651-1669.

Etyemezian, V., Davidson, C.I., Zufall, M., Dai, W., Finger, S., Striegel, M., 2000. Impingement of rain drops on a tall building. Atmospheric Environment 34, 2399-2412.

Geving, S., 1994. Averaging of climatic data and its effect on moisture transfer calculations. Norwegian Institute of Technology, Report T2-N-94/04, International Energy Agency – Annex 24 meeting, October, 1994.

Geving, S., 1997. Moisture design of building constructions. Ph.D. thesis, Norwegian University of Science and Technology, Trondheim.

Hagentoft, C.E., Kalagasidis, A.S., Adl-Zarrabi, B., Roels, S., Carmeliet, J., Hens, H., Grünewald, J., Funk, M., Becker, R., Shamir, D., Adan, O., Brocken, H., Kumaran, K., Djebbar, R., 2004. Assessment method of numerical prediction models for combined heat, air and moisture transfer in building components: benchmarks for one-dimensional cases. Journal of Thermal Envelope and Building Science 27(4), 327-352.

Hangan, H., 1999. Wind-driven rain studies. A C-FD-E approach. Journal of Wind Engineering and Industrial Aerodynamics 81, 323-331.

Hens, H. 1996. Heat, air and moisture transfer in insulated envelope parts: modelling. International Energy Agency, Annex 24. Final report, volume 1. Acco, Leuven. 1996.

Janssen, H., Blocken, B., Roels, S., Carmeliet, J., 2006a. Wind-driven rain as a boundary condition for HAM simulations: analysis of simplified modelling approaches. Building and Environment, accepted for publication.

Janssen, H., Blocken, B., Carmeliet, J., 2006b. Conservative modelling of the moisture and heat transfer in building components under atmospheric excitation. International Journal of Heat and Mass Transfer, accepted for publication.

Karagiozis, A., Hadjisophocleous, G., Cao, S., 1997. Wind-driven rain distributions on two buildings. Journal of Wind Engineering and Industrial Aerodynamics 67&68, 559-572.

Künzel, H.M., 1993. Averaging climatic data and its effect on the results of heat and moisture transfer calculations. Fraunhofer-Institut für Bauphysik, Report T1-D-93/05, International Energy Agency – Annex 24 meeting, Holzkirchen, October.

Lakehal, D., Mestayer, P.G., Edson, J.B., Anquetin, S., Sini, J.-F., 1995. Eulero-Lagrangian simulation of raindrop trajectories and impacts within the urban canopy. Atmospheric Environment 29(23), 3501-3517.

Roels, S., Vandersteen, K., Carmeliet, J., 2003. Measuring and simulating moisture uptake in a fractured porous medium. Advances in Water Resources 26, 237-246.

Sanders, C., 1996. Heat, air and moisture transfer in insulated envelope parts: Environmental conditions. International Energy Agency, Annex 24. Final report, volume 2. Acco, Leuven.

Sanders, C., Phillipson, M., 2003. UK adaptation strategy and technical measures: the impacts of climate change on buildings. Building Research and Information 31(3-4), 210-221.

Strahler, A.N., Strahler, A.H., 1984. Elements of physical geography. John Wiley & Sons.

Tang, W., Davidson, C.I., Finger, S., Vance, K., 2004. Erosion of limestone building surfaces caused by wind-driven rain. 1. Field measurements. Atmospheric Environment 38(33), 5589-5599.

Tang, W., Davidson, C.I., 2004. Erosion of limestone building surfaces caused by wind-driven rain. 2. Numerical modelling. Atmospheric Environment 38(33), 5601-5609.

van Mook, F.J.R., de Wit, M.H., Wisse, J.A., 1997. Computer simulation of driving rain on building envelopes, in: Proceedings 2nd European and African Conference on Wind Engineering (2EACWE), Genova, Italy, 1059-1066

van Mook, F.J.R., 1999. Full-scale measurements and numeric simulations of driving rain on a building, in: Proceedings 10th International Conference on Wind Engineering (10ICWE), Copenhagen, Denmark, 21-24 June, 1145-1152.

van Mook, F.J.R., 2002. Driving rain on building envelopes, Ph.D. thesis, Building Physics and Systems, Technische Universiteit Eindhoven, Eindhoven University Press, Eindhoven, The Netherlands, 198 p.

Whitaker, S., 1977. Simultaneous heat, mass and momentum transfer in porous media: a theory of drying porous media. Advances in Heat Transfer, 119-203.

Wilson, M.A., Hoff, W.D., Hall, C., 1995. Water movement in porous building materials – XIII. Absorption into a two-layer composite. Building and Environment 30, 209-219.

Wisse, J.A., 1994. Driving rain, a numerical study, in: Proceedings 9th Symposium on Building Physics and Building Climatology, Dresden, 14-16 September.

FIGURE CAPTIONS

Fig. 1. Typical example of a catch-ratio chart or η-chart that presents the catch ratio η as a function of the reference wind speed U_{10} and the horizontal rainfall intensity R_h, for a given position on the building facade and for a given wind direction. Data points are provided for a discrete set of couples (U_{10}, R_h). Intermediate values are obtained by linear interpolation (Blocken and Carmeliet, 2002).

Fig. 2. Typical images of cumuliform clouds and stratiform clouds and the resulting rainfall records: (a) Cumuliform cloud; (b) Cumuliform rain event; (c) Stratiform cloud; (d) Stratiform rain event. The measurements were made at the VLIET test site (Blocken and Carmeliet, 2005).

Fig. 3. North-west and south-west facade of the VLIET test building. The building dimensions including roof overhang length are given. The positions A and B on the facade that will be used in the present paper are indicated.

Fig. 4. Configuration of the 1D wall model used for the heat and moisture transfer simulations. Indication of the variables representing the boundary conditions (T = temperature, p = vapour pressure, e = exterior, i = interior).

Fig. 5. Moisture retention curve for the ceramic brick.

Fig. 6. Moisture (liquid and vapour) permeability as a function of the capillary pressure for the ceramic brick.

Fig. 7 (a) Cumuliform rain event: 10-minute data of the reference wind speed U_{10} and the horizontal rainfall intensity R_h. (b-c) Cumulative wind-driven rain S_{wdr} calculated with the catch-ratio charts generated by the CFD model at (b) position A and (c) position B of the VLIET building. S_{wdr} is calculated in three different ways: (1) using 10-minute data of U_{10} and R_h; (2) using arithmetically-averaged hourly data; (3) using weighted-averaged hourly data.

Fig. 8 Calculated moisture content at the outer surface of the brick wall during the rain event given in Fig. 7a for (a) position A and (b) position B of the VLIET building. The results have been calculated with three different sets of wind-driven rain data (see Fig. 7b-c).

Fig. 9 Calculated mean moisture content in the brick layer during the rain event given in Fig. 7a for (a) position A and (b) position B of the VLIET building. The results have been calculated with three different sets of wind-driven rain data (see Fig. 7b-c).

Fig. 10 (a) Stratiform rain event: 10-minute data of the reference wind speed U_{10} and the horizontal rainfall intensity R_h. (b-c) Cumulative wind-driven rain S_{wdr} calculated with the catch ratio charts generated by the CFD model at (b) position A and (c) position B of the VLIET building. S_{wdr} is calculated in three different ways: (1) using 10-minute data of U_{10} and R_h; (2) using arithmetically-averaged hourly data; (3) using weighted-averaged hourly data.

Fig. 11. Calculated moisture content at the outer surface of the brick wall during the rain event given in Fig. 10a for (a) position A and (b) position B of the VLIET building. The results have been calculated with three different sets of wind-driven rain data (see Fig. 10b-c).

Fig. 12 Calculated mean moisture content in the brick layer during the rain event given in Fig. 10a for (a) position A and (b) position B of the VLIET building. The results have been calculated with three different sets of wind-driven rain data (see Fig. 10b-c).

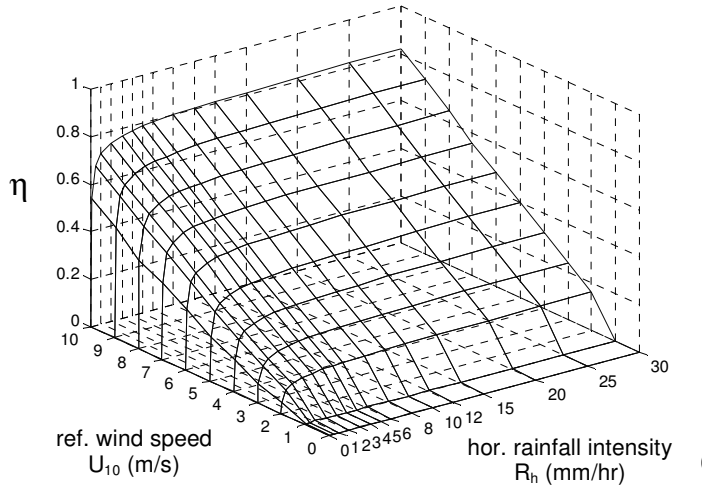

Fig. 1. Typical example of a catch-ratio chart or η-chart that presents the catch ratio η as a function of the reference wind speed U_{10} and the horizontal rainfall intensity R_h, for a given position on the building facade and for a given wind direction. Data points are provided for a discrete set of couples (U_{10}, R_h). Intermediate values are obtained by linear interpolation (Blocken and Carmeliet, 2002).

FIGURE 1

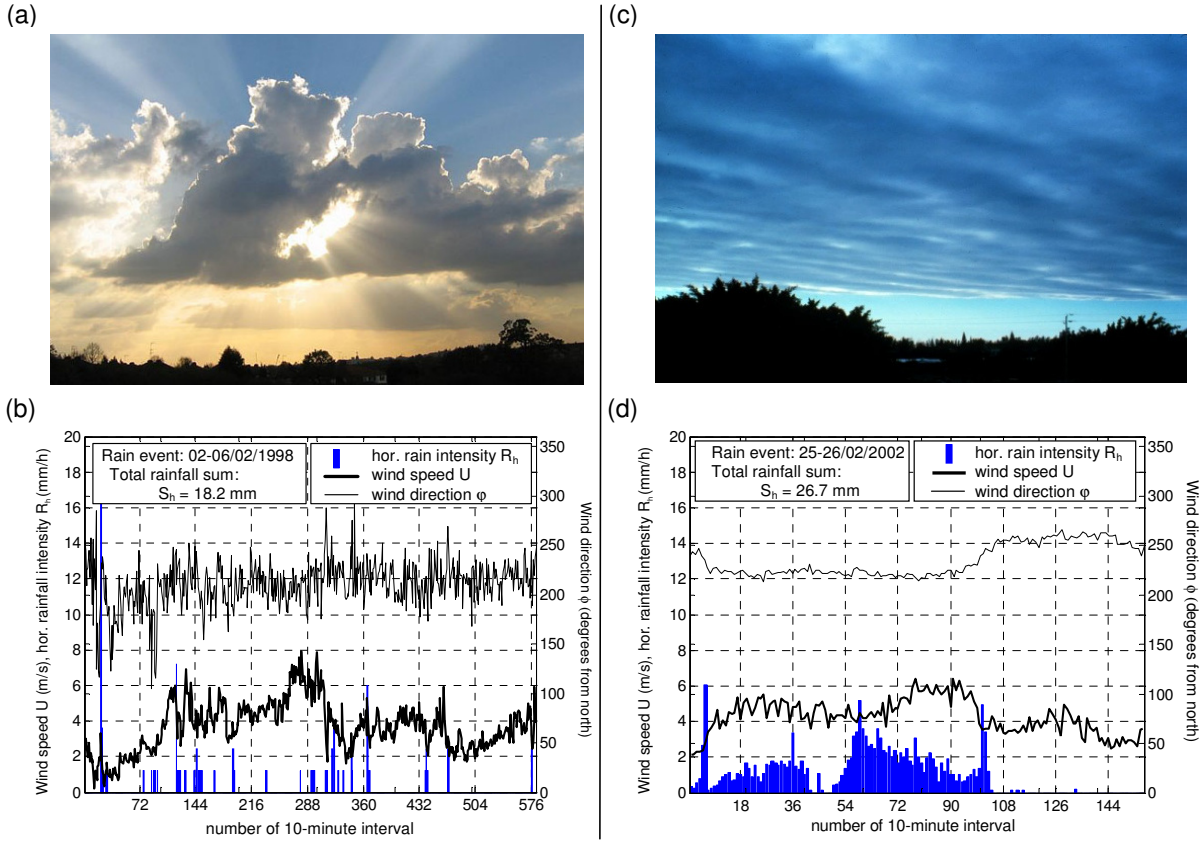

Fig. 2. Typical images of cumuliform clouds and stratiform clouds and the resulting rainfall records: (a) Cumuliform cloud; (b) Cumuliform rain event; (c) Stratiform cloud; (d) Stratiform rain event. The measurements were made at the VLIET test site (Blocken and Carmeliet, 2005).

FIGURE 2

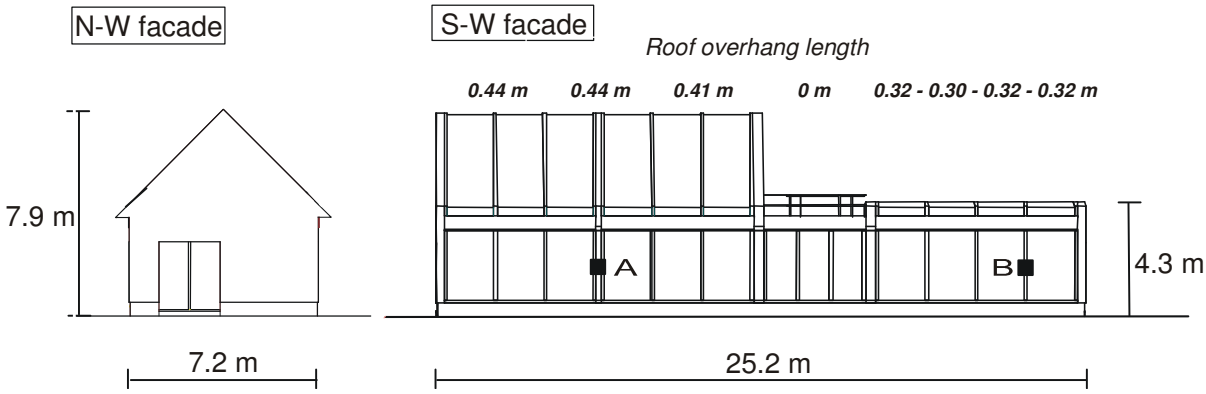

Fig. 3. North-west and south-west facade of the VLIET test building. The building dimensions including roof overhang length are given. The positions A and B on the facade that will be used in the present paper are indicated.

FIGURE 3

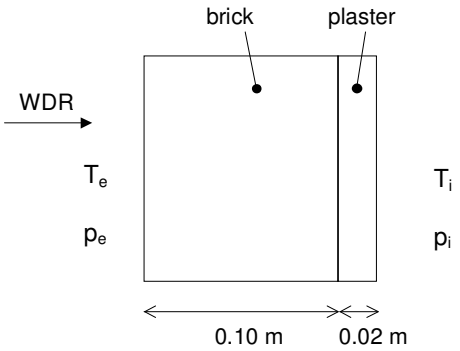

Fig. 4. Configuration of the 1D wall model used for the heat and moisture transfer simulations. Indication of the variables representing the boundary conditions (T = temperature, p = vapour pressure, e = exterior, i = interior).

FIGURE 4

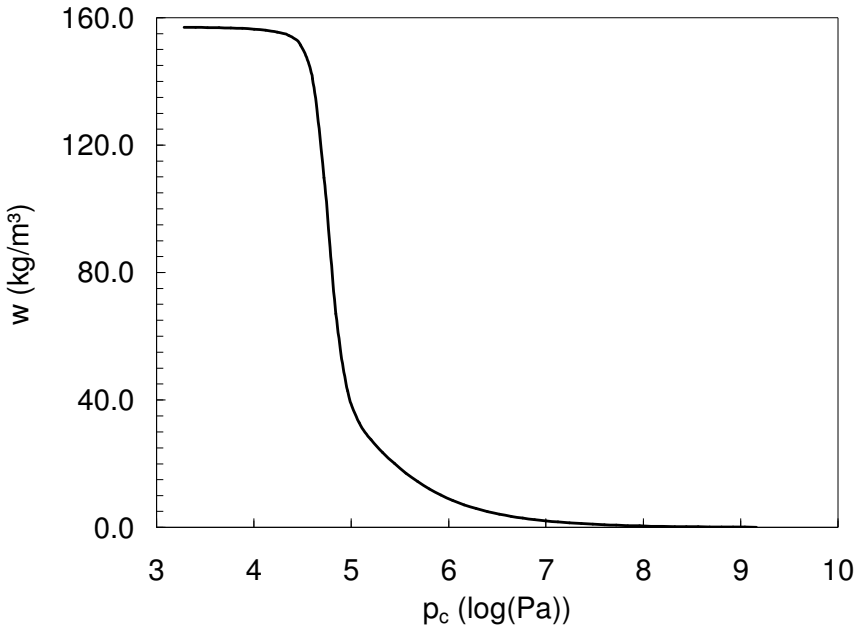

Fig. 5. Moisture retention curve for the ceramic brick.

FIGURE 5

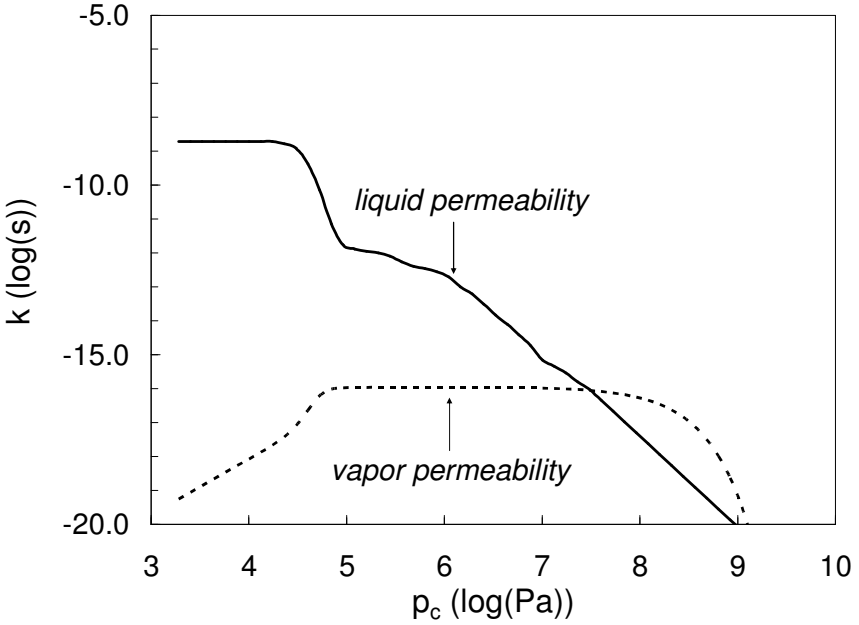

Fig. 6. Moisture (liquid and vapour) permeability as a function of the capillary pressure for the ceramic brick.

FIGURE 6

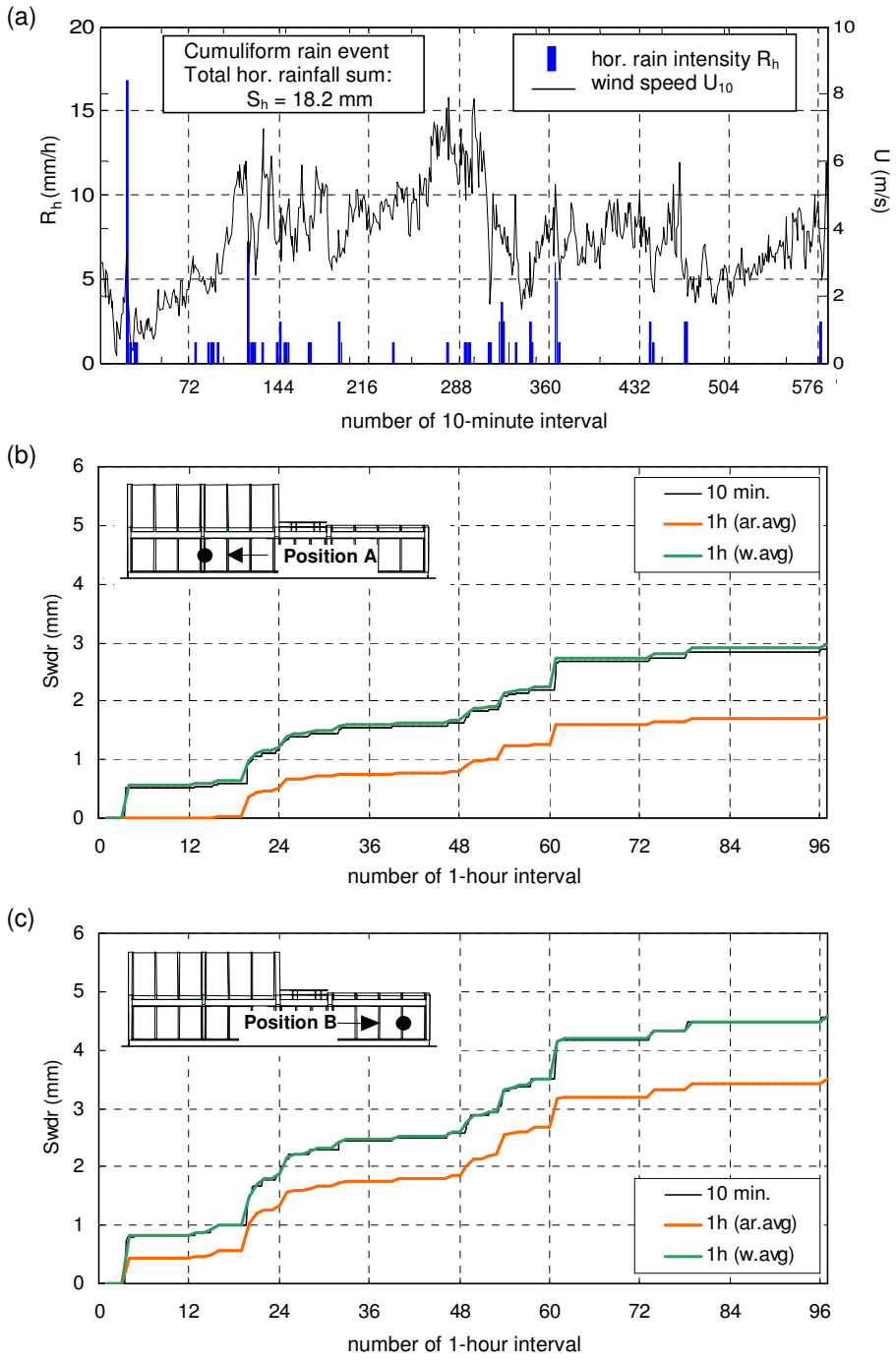

Fig. 7 (a) Cumuliform rain event: 10-minute data of the reference wind speed U_{10} and the horizontal rainfall intensity R_h. (b-c) Cumulative wind-driven rain S_{wdr} calculated with the catch-ratio charts generated by the CFD model at (b) position A and (c) position B of the VLIET building. S_{wdr} is calculated in three different ways: (1) using 10-minute data of U_{10} and R_h; (2) using arithmetically-averaged hourly data; (3) using weighted-averaged hourly data.

FIGURE 7

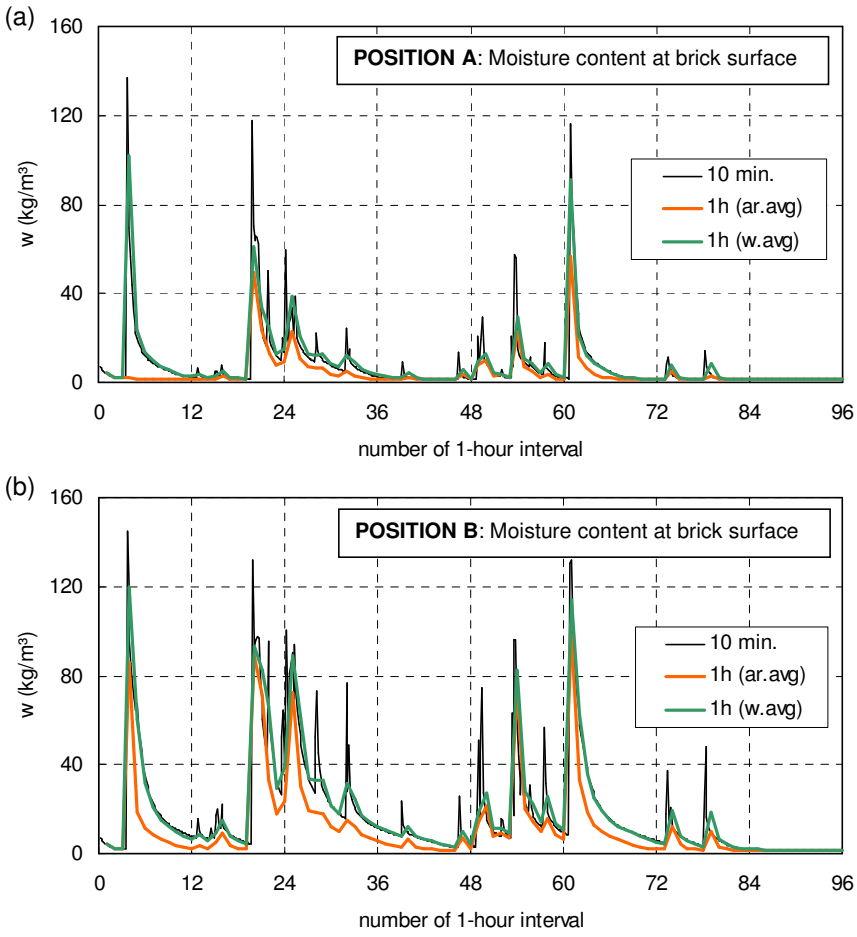

Fig. 8 Calculated moisture content at the outer surface of the brick wall during the rain event given in Fig. 7a for (a) position A and (b) position B of the VLIET building. The results have been calculated with three different sets of wind-driven rain data (see Fig. 7b-c).

FIGURE 8

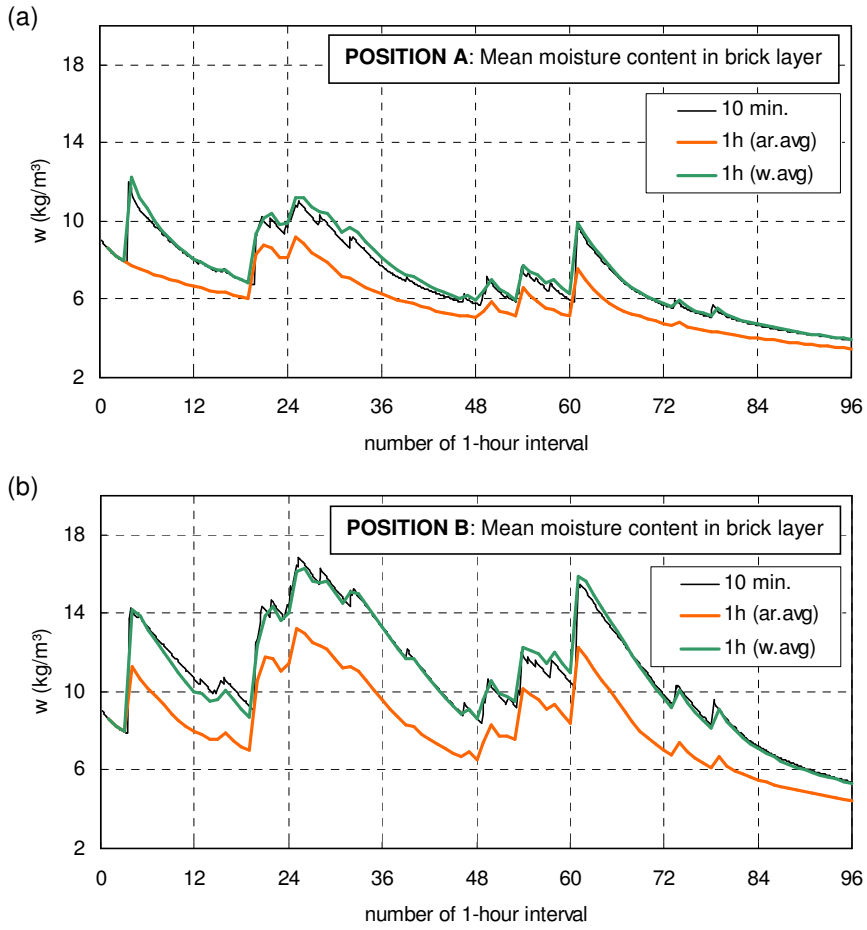

Fig. 9 Calculated mean moisture content in the brick layer during the rain event given in Fig. 7a for (a) position A and (b) position B of the VLIET building. The results have been calculated with three different sets of wind-driven rain data (see Fig. 7b-c).

FIGURE 9

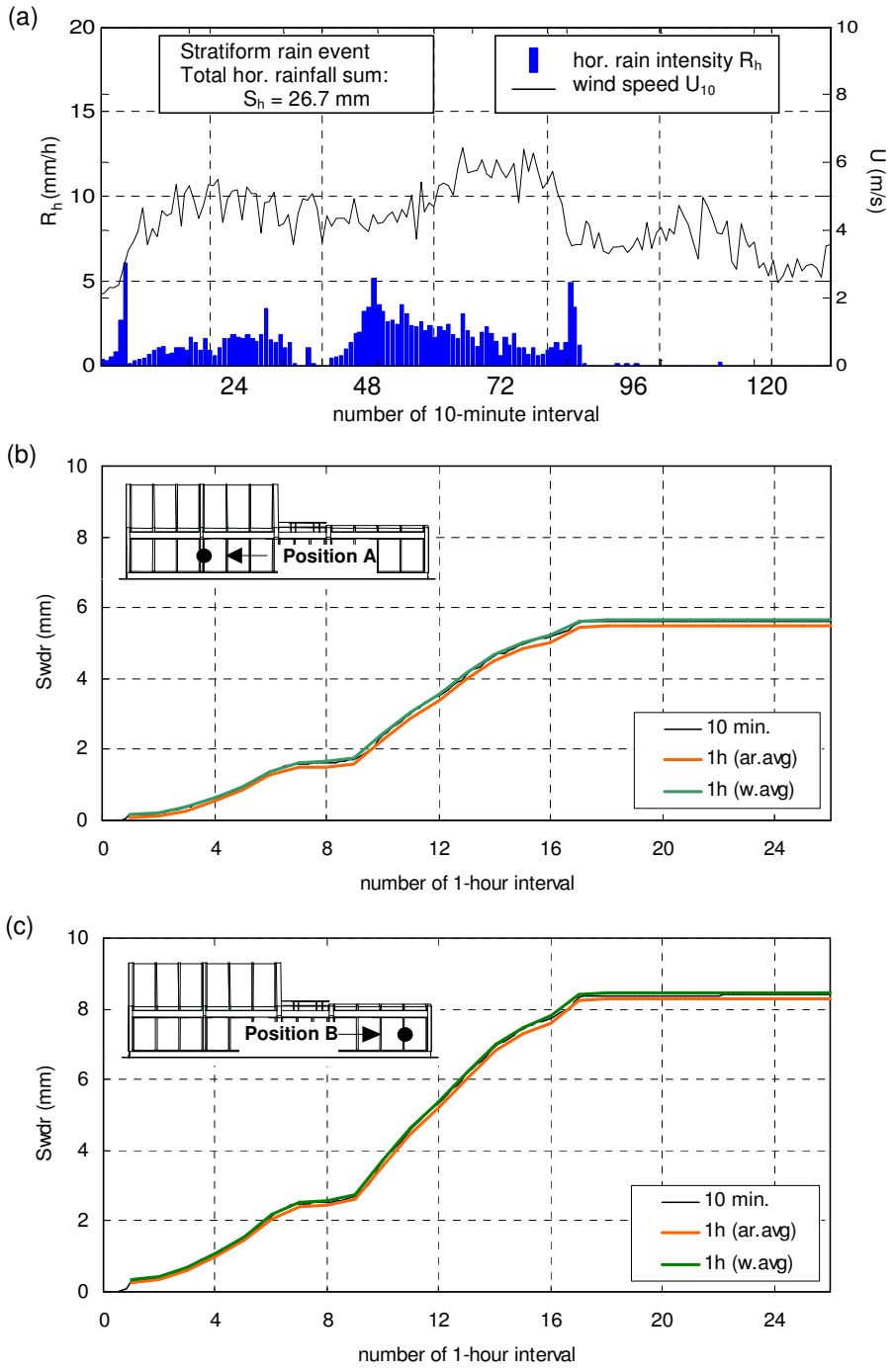

Fig. 10 (a) Stratiform rain event: 10-minute data of the reference wind speed U_{10} and the horizontal rainfall intensity R_h. (b-c) Cumulative wind-driven rain S_{wdr} calculated with the catch ratio charts generated by the CFD model at (b) position A and (c) position B of the VLIET building. S_{wdr} is calculated in three different ways: (1) using 10-minute data of U_{10} and R_h; (2) using arithmetically-averaged hourly data; (3) using weighted-averaged hourly data.

FIGURE 10

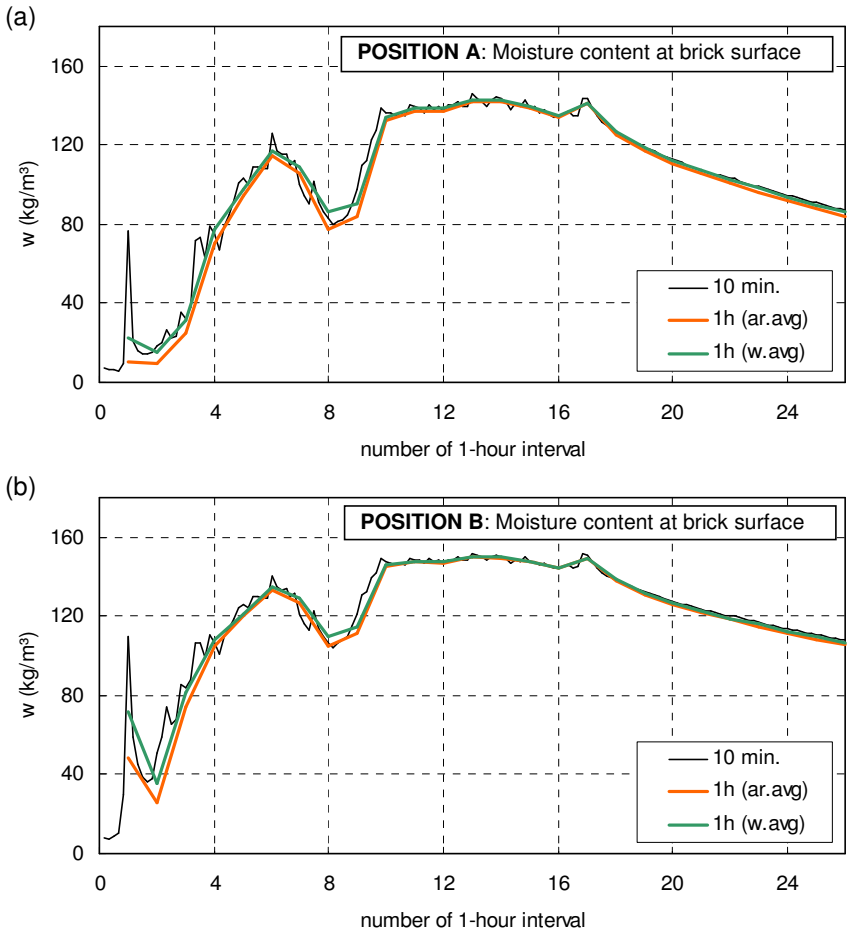

Fig. 11. Calculated moisture content at the outer surface of the brick wall during the rain event given in Fig. 10a for (a) position A and (b) position B of the VLIET building. The results have been calculated with three different sets of wind-driven rain data (see Fig. 10b-c).

FIGURE 11

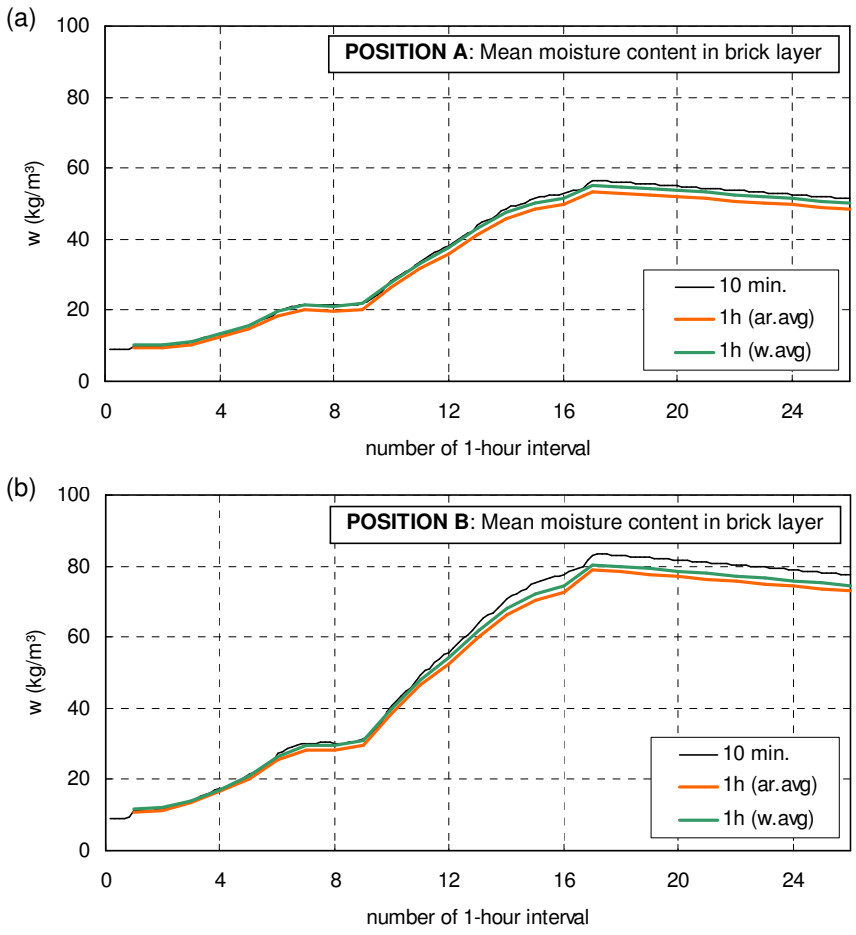

Fig. 12 Calculated mean moisture content in the brick layer during the rain event given in Fig. 10a for (a) position A and (b) position B of the VLIET building. The results have been calculated with three different sets of wind-driven rain data (see Fig. 10b-c).

FIGURE 12

Table 1: Initial and boundary conditions for the heat and moisture transfer simulations

Initial and boundary conditions		
Initial conditions		
p_c	10^6 Pa	(= 93% R.H.)
T	Linear from 283 K at outer surface to 293 K at inner surface	
Boundary conditions		
heat		
T_e	283 K	
T_i	293 K	
h_e	25 W/m²K	
h_i	8 W/m²K	
moisture		
p_e	1227 Pa	(= 90% R.H.)
p_i	1402 Pa	(= 60% R.H.)
β_e	$1x10^{-7}$ s/m	
β_i	$3x10^{-8}$ s/m	
T_{wdr}	283 K	